



Investigation of the Effect of Nano Powder Mixed Dielectric on EDM Process

Rasha R. Elias^{a*}

^a Dept. of Production Engineering and Metallurgy, University of Technology, Baghdad, Iraq.
70166@uotechnology.edu.iq

*Corresponding author.

Submitted: 02/06/2019

Accepted: 30/07/2019

Published: 25/03/2020

KEY WORDS

Artificial Neural Network, Electrical Discharge Machining, Metal Removal Rate, Minitab software, Nano powder.

ABSTRACT

In this paper, Artificial Neural Network was adopted to predict the effect of current, the concentration of aluminum oxide (Al_2O_3) and graphite Nanopowders in dielectric fluid for the machining of Carbon steel 304 using Electrical Discharge Machining (EDM). The process variables were utilized to find their effect on Material Removal Rate (MRR), Surface Roughness (SR), and Tool Wear Rate (TWR). It was revealed from the experimental work that the addition of aluminum oxide and graphite Nanopowders into dielectric fluid maximizing MRR, minimized the SR and TWR at various variables. Minitab software was used in the design of experiments. Analysis of the process outputs of EDM indicates that graphite powder concentration greatly influencing SR also the discharge current whereas the current and Nanopowders concentration has more percentage of influence on the TWR and MRR.

How to cite this article: R. R. Elias, "Investigation of the effect of nano powder mixed dielectric on EDM process," *Engineering and Technology Journal*, Vol. 38, Part A, No. 03, pp. 295-307, 2020.

DOI: <https://doi.org/10.30684/etj.v38i3A.337>

This is an open access article under the CC BY 4.0 license <http://creativecommons.org/licenses/by/4.0>.

1. Introduction

The EDM is one of the non-traditional machining operations that used to machine electrically conductive and extra hard metals for producing molds, dies, automotive, aerospace, and surgical parts. A series of electric sparks between an electrode (tool) and the machined material in this operation controlled the removal process by erosion. The thermal energy of the sparks generates extreme heat power on the machined, causing the melting and vaporizing of machined material. EDM technique is low machining efficiency and poor surface quality sometimes. Therefore, powder mixed EDM (PMEDM) or the existence of powders added to the dielectric fluid is used. The electrically conductive powder minimizes the strength of the insulation of the dielectric and maximizing the spark gap between the electrode and machined surface, which gave better machining and maximized metal removal rate (MRR) and surface quality [1]. Due to the rapid tempering melting and cooling process, subsurface defects such as cracks, residual stress, spalling, metallurgical

properties, heat-affected zones, and porosity are commonly observed on the structure of the part. The technique of introducing Nanopowder into EDM fluid called the powder or Nanopowder mixed EDM (PMEDM) is introduced to keep the machining specifications and overcome the part drawbacks. Despite of the wide improvements gained by PMEDM, the importance of the effect of introducing powder in fluid in PMEDM processes on surface quality, part precise and machining time still needing improvement and investigation. Introducing of powders in the fluid in PMEDM together with high ratios of powder in the dielectric fluid was noticed as an excellent way to maximize surface finish and minimize machining time. The powder electrical conductivity leads to maximizing the overall fluid conductivity, then minimizing the strength of the dielectric of the fluid and enlarging the gap distance between the tool and the machined surface. Maximizing the gap together with the high concentricity of particles in the dielectric improves the discharging process to be more accurate and minimizes the need to back off the tool because of arcing and short-circuiting, which gives minimum machining time [2]. In addition, researches revealed that the addition of graphite powders in kerosene for using as the dielectric medium results from improvement in Tool wear rate and metal removal rate [3].

Rana et al. makes a review of the trends of the EDM technique by using powder mixed dielectric and water as dielectric fluid. EDM has been adopted to enhance surface properties utilizing many electrodes and by introducing many powders to the fluid. The majority of the works focused on Al, Si, and graphite powders and some with other types of powder-like Cr, Ni, Mo, the presence of particles of metal in the fluid converts its properties, which minimizing the insulation of the fluid and maximizing the spark between the tool and machined surface. Most of the published studies on mixed dielectric have investigated the role of such technologies on MRR, surface finish, and TWR [4].

Tseng et al. chooses copper, silver, and titanium as the targets to reveal the relation between Nanofluids properties and (electrical discharge machining EDM) technique. UV-visible spectroscopy (UV-Vis) was adopted to find the concentricity distribution of Nanofluids; zeta-size analysis is utilized for finding Zeta-Potential, Nano metal particles, and the size distribution of nanoparticles in the fluid. Depending on the outputs, the control of pulse duration in addition to the concentricity of liquid and heat in the process influencing the size of the metal particles after the process. Finally, many tools like the scanning electron microscope were utilized to reveal the size, shape, and metal structure composition after processing [5].

Abdul Razak et al. a comparison of (Electrical Discharge Machining EDM) on Reaction Bonded Silicon Carbide (RB-SiC) adopting several kinds of additives and surfactants has been done. The minimum Smell (LS) EDM oil used practically was mixed with many surfactants, namely Span 20, Span 80, Span 83, and Span 85. The powders that used to manipulates the work were Carbon Nanofiber, Carbon Powder, and Carbon NanoPowder. These additives are unlike in terms of shape and size. The output indicates that the surfactant and powders added dielectric fluid not only influencing the spark gap and MR, but also minimize the EWR. Therefore, the discharge frequency maximized, resulting in a higher MRR and spark gap [6].

Boopathi, et al. electrical discharge machining characteristics of Inconel 718 alloy using titanium carbide (TiC) nanoparticles mixed dielectric fluid was studied. Experiments have been performed according to face-centered central composite design. The effect of input parameters such as pulse-on-time, pulse-off-time, and current on the output responses like MRR, TWR, and Ra are evaluated. The result shows that MRR and Ra get improved, TWR get reduced [7].

2. Artificial Neural Network

The mathematical model in the present work is determined to utilize ANN for each output separately. It was needed to adopt a mathematical model to control the response in terms of cutting variables. ANN is a multilayered diagram made up of one or more layers placed between input and output layers. Layers consist of many processing parts called neurons. They are connected with variable weights to be estimated. In the network, each part or neuron gains total information from all of the others in the previous layer as [8]:

$$net_j = \sum_{i=0}^N w_{ij} x_i \quad (1)$$

Where N is the number of inputs, x_i is the i th input to the j th neuron in the hidden layer, w_{ij} is the weight of i th input and net_j is the total or net input. A neuron in the net gives its results (out_j) by processing the input of the net through an activating function f , hyperbolic function adopted in this study as below:

$$out_j = f(net_j) = \frac{1 - e^{-net_j}}{1 + e^{-net_j}} \quad (2)$$

In reducing a combination of errors and determining the suitable build to produce a well-total network, the Bayesian regularization back-propagation based on Levenberg –Marquardt algorithm was adopted for training of the net using MATLAB Neural Network Toolbox. The set of experimental data contains 27 experiments where the training subset includes 21 experiments of the data, while the testing group includes 6 experiments. The step-by-step mode of training was adopted for the network. The most suitable model with a 3-5-1 layout was found to be good for this work.

Back Propagation learning algorithm updates the weights and trains the NN until the mean square error (MSE) converges to a minimum value between the network and desired output [9]:

$$MSE = \frac{1}{km} \sum_{m=1}^M \sum_{k=1}^K (DES_{mk} - OUT_{mk})^2 \quad (3)$$

Where DES_{mk} and OUT_{mk} are the desired output and the network output, K is the number of output neurons; M is the overall number of data set. In estimations of weights variables, often called as network training, the weights are given quasi-random, intelligently chosen initial values. They are then iteratively updated until convergence to certain values using the gradient descent method. This method updates weights to reduce the MSE between training data and network prediction as below [8]:

$$w_{ij}^{new} = w_{ij}^{old} + \Delta w_{ij} \quad (4)$$

$$\Delta w_{ij} = -\frac{\partial E}{\partial w_{ij}} out_j \quad (5)$$

Where E is the MSE and out_j is the j th neuron output. η is the parameter of the learning rate controlling the stability and rate of convergence of the network. The learning rate η , which is a constant between 0 and 1, is chosen to be 0.001. In order to measure the accuracy of the prediction model, percentage error ϕ_i and average percentage error $\bar{\phi}$ were used and defined as [9]:

$$\phi_i = \frac{|R_{aie} - R_{aip}|}{R_{aie}} \times 100\% \quad (6)$$

Where:

ϕ_i = Each experiment percentage error.

R_{aie} = Experimental Ra, MRR or TWR.

R_{aip} = Predicted Ra, MRR or TWR.

$$\bar{\phi} = \frac{\sum_{i=1}^m \phi_i}{m} \quad (7)$$

$\bar{\phi}$ = average percentage error

m = No. of experiments.

3. Experimental Work

I. Selection of tool and work materials

In this work, Carbon steel 304 has been chosen as the workpiece. Twenty-seven specimens with dimensions around (40 mm x 40mm x4mm), as shown in Figure 1, have been used, which is inspected in [the state company for inspection and engineering rehabilitation] / (Lab. and engineering inspection Dept.). The chemical composition and material properties of Carbon steel 304 are shown in Tables 1 and 2. The selected electrode was Copper with a 10 mm diameter and 80 mm length due to its high conductive electrical and thermal properties.

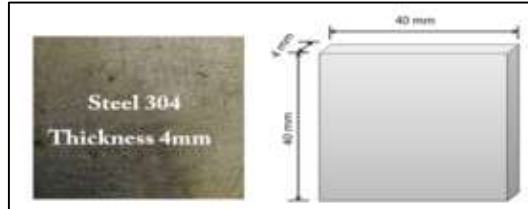


Figure 1: work piece material with dimensions

Table 1: Chemical composition of workpiece

| Material | Used SS 304 |
|----------|-------------|
| C % | 0.08 |
| Mg % | 2.00 |
| P % | 0.045 |
| S % | 0.03 |
| Si % | 0.75 |
| Cr % | 18 - 20 |
| Ni % | 8 - 10.5 |
| N % | 0.10 |
| Fe % | balance |

Table 2: Mechanical properties of work piece material

| Grade | Used SS 304 |
|--|-------------|
| Tensile strength (MPa) Min | 515 |
| Hardness Brinell (HB) Max | 201 |
| Density (Kg/m ³) | 8000 |
| Elastic Modulus (GPa) | 193 |
| Thermal conductivity (W/m.K) At 100 °C | 16.2 |
| At 500 °C | 21.5 |
| Electrical Resistivity (nΩm) | 720 |

II. Preparation of Nanopowders

Figure 2, shows the micrographs of Nano Al₂O₃ composites with (10 - 20) nm, produced by semi-solid casting and graphite Nanopowder with (20 - 40) nm. The test has been done on FE-SEM Hitachi S-4160 with a scale bar 300 nm.

III. Selection of parameters

There are many input variables to be included in the EDM process for calculating the optimum process response. Based on the researches, it was revealed that the variables such as graphite powder, current, and Al₂O₃ concentration have a direct effect on the EDM response. Before manipulating the main EDM tests, many empirical experiments have been done in order to find a suitable range for the input variables. It was revealed that MRR was maximized when a current of more than 15 Amp adopted, which make the selection of about this value necessary. Also, introducing the graphite powder with about (3 to 9 g/lit) into the fluid to reveal the influence on MRR and SR. Al₂O₃ concentration changed between (4 g/lit and 12 g/lit), while the other factors kept constant. The range of other process parameters is illustrated in Table 3.

IV. Design of experiments

The number of experiments significantly needed to be influenced by the design of experimentation. For this reason, experiments must be carefully distributed. In this work, many machining tests (27 experiments) depend on a full factorial with three-level design (3^3) was utilized to reveal surface quality, tool wear ratio and MRR. The selected OA, and cutting parameters levels are illustrated in Table 4.

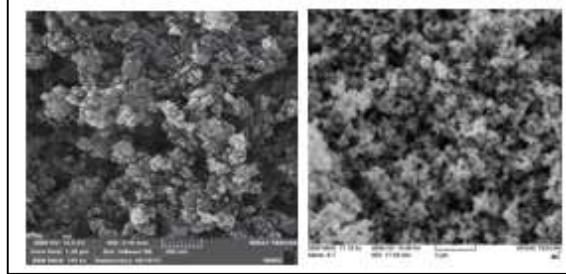


Figure 2: (a) Nano Al_2O_3 with (10 - 20) nm and (b) Nano graphite powder with (20 - 40) nm

Table 3: Selected parameters and their levels

| Code | Parameter | Levels | | |
|------|---|--------|---|---|
| | | 1 | 2 | 3 |
| A | Current (A) | 1 | 1 | 2 |
| | | 0 | 5 | 0 |
| B | Al_2O_3 concentration (g/L) | 4 | 8 | 1 |
| | | | | 2 |
| C | Graphite concentration (g/L) | 3 | 6 | 9 |

Table 4: Coded cutting parameters and real values

| E. | Coded Values | | | Real Values | | |
|----|--------------|---|---|-------------|------------------------------|---------------|
| | A | B | C | Current | Al_2O_3 Con. | Graphite Con. |
| 1 | 1 | 1 | 1 | 10 | 4 | 3 |
| 2 | 1 | 1 | 2 | 10 | 4 | 6 |
| 3 | 1 | 1 | 3 | 10 | 4 | 9 |
| 4 | 1 | 2 | 2 | 10 | 8 | 6 |
| 5 | 1 | 2 | 3 | 10 | 8 | 9 |
| 6 | 1 | 2 | 1 | 10 | 8 | 3 |
| 7 | 1 | 3 | 3 | 10 | 12 | 9 |
| 8 | 1 | 3 | 1 | 10 | 12 | 3 |
| 9 | 1 | 3 | 2 | 10 | 12 | 6 |
| 10 | 2 | 1 | 2 | 15 | 4 | 6 |
| 11 | 2 | 1 | 3 | 15 | 4 | 9 |
| 12 | 2 | 1 | 1 | 15 | 4 | 3 |
| 13 | 2 | 2 | 3 | 15 | 8 | 9 |
| 14 | 2 | 2 | 1 | 15 | 8 | 3 |
| 15 | 2 | 2 | 2 | 15 | 8 | 6 |
| 16 | 2 | 3 | 1 | 15 | 12 | 3 |
| 17 | 2 | 3 | 2 | 15 | 12 | 6 |
| 18 | 2 | 3 | 3 | 15 | 12 | 9 |
| 19 | 3 | 1 | 3 | 20 | 4 | 9 |
| 20 | 3 | 1 | 1 | 20 | 4 | 3 |
| 21 | 3 | 1 | 2 | 20 | 4 | 6 |
| 22 | 3 | 2 | 1 | 20 | 8 | 3 |
| 23 | 3 | 2 | 2 | 20 | 8 | 6 |
| 24 | 3 | 2 | 3 | 20 | 8 | 9 |

| | | | | | | |
|----|---|---|---|----|----|---|
| 25 | 3 | 3 | 2 | 20 | 12 | 6 |
| 26 | 3 | 3 | 3 | 20 | 12 | 9 |
| 27 | 3 | 3 | 1 | 20 | 12 | 3 |

4. Results and Discussion

Table 5 explains the experimental readings of machining Carbon steel 304 depending on L27 (33) mixed orthogonal array. The process outputs, Ra in μm , tool wear rate (mm^3/min), and metal removal rate (mm^3/min) has been measured and evaluated.

Table 5: Experimental readings of machining Carbon steel 304 depending

| E. | Current | Al ₂ O ₃ Con. | E. | Current | Al ₂ O ₃ Con. |
|----|---------|-------------------------------------|----|---------|-------------------------------------|
| 1 | 10 | 4 | 1 | 10 | 4 |
| 2 | 10 | 4 | 2 | 10 | 4 |
| 3 | 10 | 4 | 3 | 10 | 4 |
| 4 | 10 | 8 | 4 | 10 | 8 |
| 5 | 10 | 8 | 5 | 10 | 8 |
| 6 | 10 | 8 | 6 | 10 | 8 |
| 7 | 10 | 12 | 7 | 10 | 12 |
| 8 | 10 | 12 | 8 | 10 | 12 |
| 9 | 10 | 12 | 9 | 10 | 12 |
| 10 | 15 | 4 | 10 | 15 | 4 |
| 11 | 15 | 4 | 11 | 15 | 4 |
| 12 | 15 | 4 | 12 | 15 | 4 |
| 13 | 15 | 8 | 13 | 15 | 8 |
| 14 | 15 | 8 | 14 | 15 | 8 |
| 15 | 15 | 8 | 15 | 15 | 8 |
| 16 | 15 | 12 | 16 | 15 | 12 |
| 17 | 15 | 12 | 17 | 15 | 12 |
| 18 | 15 | 12 | 18 | 15 | 12 |
| 19 | 20 | 4 | 19 | 20 | 4 |
| 20 | 20 | 4 | 20 | 20 | 4 |
| 21 | 20 | 4 | 21 | 20 | 4 |
| 22 | 20 | 8 | 22 | 20 | 8 |
| 23 | 20 | 8 | 23 | 20 | 8 |
| 24 | 20 | 8 | 24 | 20 | 8 |
| 25 | 20 | 12 | 25 | 20 | 12 |
| 26 | 20 | 12 | 26 | 20 | 12 |
| 27 | 20 | 12 | 27 | 20 | 12 |

I. Results for MRR

Figures 3 and 4 show the output of 27 value of MRR in the experiments. Twenty-one reading was adopted to train the net; the rest of the data (six readings) were adopted to test the trained net. The relation between the 21 values gained from experiments and the predicted reading plotted in Figure 3. It can be revealed from this figure that the practical values have come ahead to the predicted. Figure 4 indicates that good correspond can be noticed between the test and measured values. Table 6 indicates the results predicted from training the net compared with experimental results for MRR. The maximum value of MRR was ($5.93 \text{ mm}^3/\text{min}$) in Table 6 at current (20 A), Al₂O₃ concentration (12 g/l), and graphite concentration (9 g/l). MRR increases with increasing current. When graphite particles are supplied to the fluid, the particles of powder get energized and move in a zigzag motion when applied to the voltage. They produce a chain in the machining gap. This chain is bridging the gap between the machined surface and the tool. As the current maximized, the energy also increased. Hence, the high energy leads to elevated melting ranges; it causes high precipitant force and high

evaporation acting on the machined region related to maximum MRR. The frequency of sparking is maximized with better flushing of wrack effectively away from the gap. This produced an effective discharge transmissivity under the sparking area due to maximum heat conductivity. Hence, MRR maximized in powder mixed dielectric fluid. The data set is consisting of six MRR values selected randomly from 27 MRR experiments, which were not used for the training of ANN. Table 7 illustrates the data tested for MRR. It can be revealed that the predicted error for the data set is found to be 4.61%, i.e., while accuracy is 95.39%, and the MSE is 0.0378. It can be seen from Figure 5, the regression coefficient for the training set is equal to 1, which shows that there is an exact linear relationship between the targets and the output.

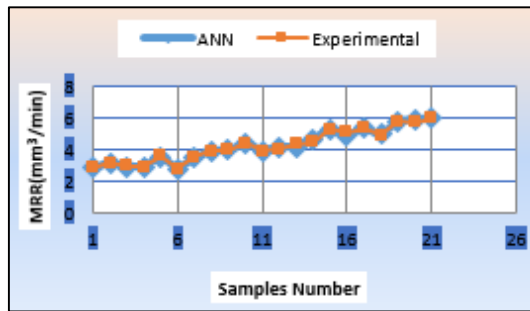


Figure 3: Measured values compared with predicted MRR values for training set

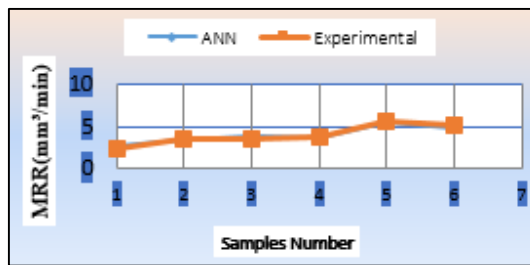


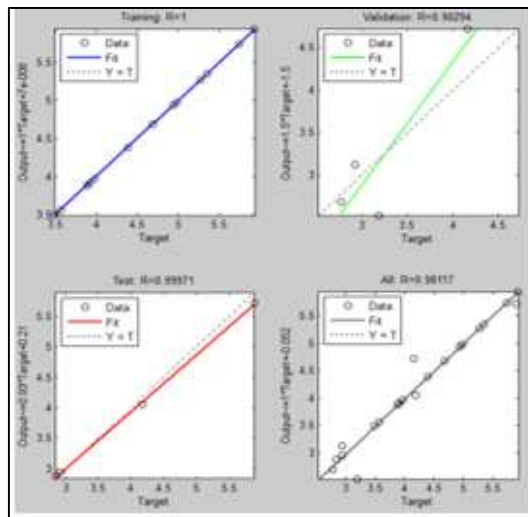
Figure 4: The measured values compared with the predicted of MRR for testing set

Table 6: Results predicted from training the net

| E. | Current | Al ₂ O ₃ Con. | MRR (mm ³ /min) | | |
|----|---------|-------------------------------------|----------------------------|----------|-----------|
| | | | Graphite Con. | Measured | Predicted |
| 1 | 10 | 4 | 6 | 2.84 | 2.87 |
| 2 | 10 | 4 | 9 | 3.19 | 3.18 |
| 3 | 10 | 8 | 6 | 2.93 | 2.95 |
| 4 | 10 | 8 | 3 | 2.93 | 2.94 |
| 5 | 10 | 12 | 9 | 3.56 | 3.58 |
| 6 | 10 | 12 | 3 | 2.78 | 2.78 |
| 7 | 10 | 12 | 6 | 3.49 | 3.51 |
| 8 | 15 | 4 | 6 | 3.88 | 3.91 |
| 9 | 15 | 4 | 9 | 3.96 | 3.96 |
| 10 | 15 | 8 | 9 | 4.38 | 4.39 |
| 11 | 15 | 8 | 3 | 3.91 | 3.90 |
| 12 | 15 | 8 | 6 | 4.18 | 4.06 |
| 13 | 15 | 12 | 6 | 4.16 | 4.37 |
| 14 | 15 | 12 | 9 | 4.68 | 4.48 |
| 15 | 20 | 4 | 9 | 5.27 | 5.29 |
| 16 | 20 | 4 | 3 | 4.93 | 5.07 |
| 17 | 20 | 4 | 6 | 5.35 | 5.35 |
| 18 | 20 | 8 | 3 | 4.98 | 4.88 |
| 19 | 20 | 8 | 9 | 5.74 | 5.74 |
| 20 | 20 | 12 | 6 | 5.89 | 5.72 |
| 21 | 20 | 12 | 9 | 5.93 | 5.93 |

Table 7: Results predicted from testing the net

| E. | A | B | C | MRR (mm ³ /min) | | Err % | ANN results | | |
|----|----|----|---|------------------------------|-------|-------|----------------|--------|--------|
| | | | | Meas. | Pred. | | $\bar{\phi}$ % | MSE | Acc. % |
| 1 | 10 | 4 | 3 | 2.46 | 2.67 | 8.54 | 4.6 | 0.0378 | 95.3 |
| 2 | 10 | 8 | 9 | 3.47 | 3.47 | 0 | | | |
| 3 | 15 | 4 | 3 | 3.63 | 3.81 | 4.96 | | | |
| 4 | 15 | 12 | 3 | 3.83 | 3.61 | 5.74 | | | |
| 5 | 20 | 8 | 6 | 5.62 | 5.42 | 3.56 | | | |
| 6 | 20 | 12 | 3 | 5.14 | 4.89 | 4.86 | | | |

**Figure 5: Regression graphs for MRR**

II. Results for TWR

Figures 6 and 7 illustrates the results of 27 reading for TWR with the number of experiments. Twenty-one reading of TWR was used to train the net, while the rest of the data (six reading) used for testing the trained net. The relation between the 21 reading gained from tests and those predicted from the net illustrated in Figure 6. It can be concluded that the measured TWR values were too near to the predictions. From Figure 7, the relation between the six measured and predicted values of TWR indicates a good agreement between these values. Table 8 presents the predicted results from training the net compared with practical values. The data set is consisting of 21 TWR values selected from 27 tests. The minimum value was (0.8 mm³/min) in Table 8 at current (10A), AL₂O₃ concentration (4g/l), and graphite concentration (6g/l). It can be observed that TWR minimized by maximizing the concentration of graphite powder. Because of adding graphite particles, uniform distribution of energy and good conductivity of discharge gained in nominal TWR. Table 9 shows the results gained from the testing of the trained net compared with practical results. The data set is consisting of six values selected randomly from 27 TWR tests, which were not utilized for training of net. It can be noticed that the predicted error for the data set is found to be 5.03%, i.e., the accuracy is 94.97%, and the MSE is 0.0085. It can be seen from Figure 8; the regression coefficient for the training set is to be approximately 1; this indicates that there is an exact linear relationship between outputs and targets.

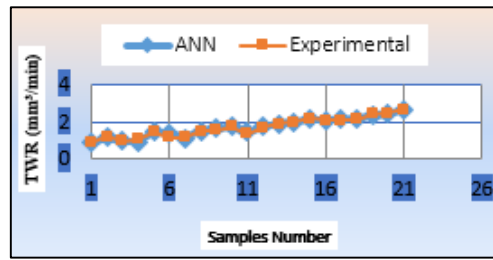


Figure 6: Measured values compared with predicted TWR values for training set

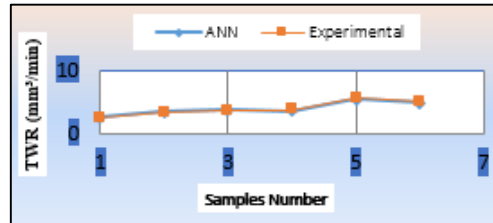


Figure 7: The measured values compared with the predicted TWR values for testing set

Table 8: Results predicted from training the net

| E. | Current | Al ₂ O ₃ Con. | Graphite Con. | TWR (mm ³ /min) | |
|----|---------|-------------------------------------|---------------|-----------------------------|-----------|
| | | | | Measured | Predicted |
| 1 | 10 | 4 | 6 | 0.86 | 0.86 |
| 2 | 10 | 4 | 9 | 1.19 | 1.21 |
| 3 | 10 | 8 | 6 | 0.97 | 0.99 |
| 4 | 10 | 8 | 3 | 0.95 | 1.09 |
| 5 | 10 | 12 | 9 | 1.48 | 1.46 |
| 6 | 10 | 12 | 3 | 1.39 | 1.19 |
| 7 | 10 | 12 | 6 | 1.14 | 1.15 |
| 8 | 15 | 4 | 6 | 1.49 | 1.49 |
| 9 | 15 | 4 | 9 | 1.67 | 1.57 |
| 10 | 15 | 8 | 9 | 1.75 | 1.77 |
| 11 | 15 | 8 | 3 | 1.48 | 1.38 |
| 12 | 15 | 8 | 6 | 1.74 | 1.69 |
| 13 | 15 | 12 | 6 | 1.88 | 1.91 |
| 14 | 15 | 12 | 9 | 1.97 | 2.01 |
| 15 | 20 | 4 | 9 | 2.16 | 2.17 |
| 16 | 20 | 4 | 3 | 2.07 | 2.07 |
| 17 | 20 | 4 | 6 | 2.12 | 2.07 |
| 18 | 20 | 8 | 3 | 2.17 | 2.14 |
| 19 | 20 | 8 | 9 | 2.31 | 2.41 |
| 20 | 20 | 12 | 6 | 2.44 | 2.46 |
| 21 | 20 | 12 | 9 | 2.67 | 2.65 |

Table 9: Results predicted from testing the net

| E. | A | B | C | TWR (mm ³ /min) | | Err % | ANN results | | |
|----|----|----|---|------------------------------|-------|-------|----------------|-------|--------|
| | | | | Meas. | Pred. | | $\bar{\phi}$ % | MSE | Acc. % |
| 1 | 10 | 4 | 3 | 0.91 | 0.95 | 4.39 | 5.03 | 0.008 | 94.97 |
| 2 | 10 | 8 | 9 | 1.26 | 1.32 | 4.76 | | | |
| 3 | 15 | 4 | 3 | 1.36 | 1.31 | 3.68 | | | |
| 4 | 15 | 12 | 3 | 1.56 | 1.43 | 8.33 | | | |
| 5 | 20 | 8 | 6 | 2.21 | 2.27 | 2.71 | | | |
| 6 | 20 | 12 | 3 | 2.37 | 2.22 | 6.33 | | | |

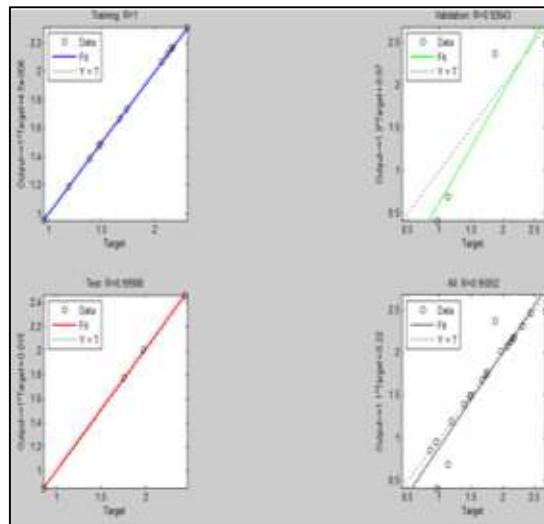


Figure 8: Regression graphs for TWR

III. Results for Ra

The results of 27 reading for Ra from the number of experiments illustrated in Figures 9 and 10. Twenty-one reading was used for the net training, while the rest of the data (six reading) were used for testing the trained net. The relation between the 21 reading gained from tests and those predicted from the model is illustrated in Figure 9. It can be observed from this figure that the measured Ra values were closed to the predicted values. From Figure 10, the relation between the six measured and predicted values of Ra indicates a good agreement between these values. Table 8 presents the predicted results from training the net compared with the experimental results of Ra. The minimum value of Ra was (1.36 μm) in Table 10 at current (10 A), Al_2O_3 concentration (12 g/l), and graphite concentration (9 g/l). The surface quality is related to the current, which affects evaporation, melting, and exhaust removal of material. Minimum current leads to low energies. Minimum energies are responsible for minimum impulse forces, on the discharge zone, and for the formation of small craters on the machined surface producing high surface quality. Graphite powder suspended into fluid easily collapses the insulation, which minimize the electrical resistivity of the fluid and maximizing the discharge gap, which leads to minimizing the impulse force of the discharge channel. This effect on the machining gap minimizes the plasma channel (high heat transfer) from the workpiece to the tool, which maximizes the material removal rate. The machined surface indicates uneven sizes of craters, which caused low surface finish. Al_2O_3 powder addition works as polishing to the surface, which gives a better surface finish. Table 11 indicates the outputs of the testing of the trained net model compared with practical readings. The data is consisting of six Ra values selected from 27 Ra measurements, which were not used for training of ANN. Table 11 presents the test data for Ra. It can be noticed that the predicted error for the data set is found to be 4.98%, i.e., the accuracy is 95.2%, and the MSE is 0.0164. It can be seen from Figure 11, the regression coefficient for the training set is to be approximately 1; this indicates that there is an exact linear relationship between outputs and targets.

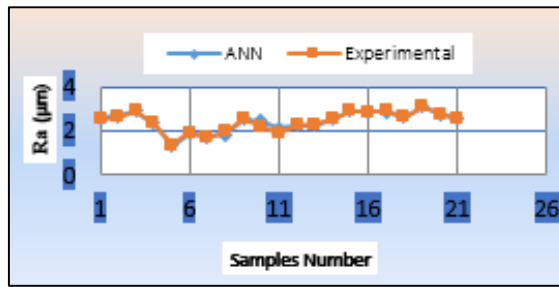


Figure 9: The measured values compared with predicted Ra for training set

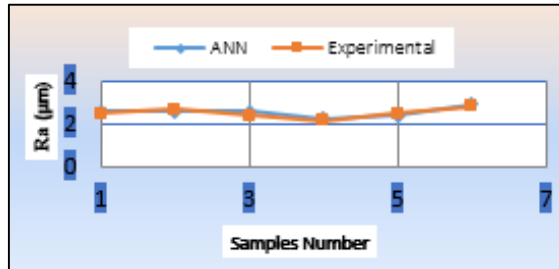


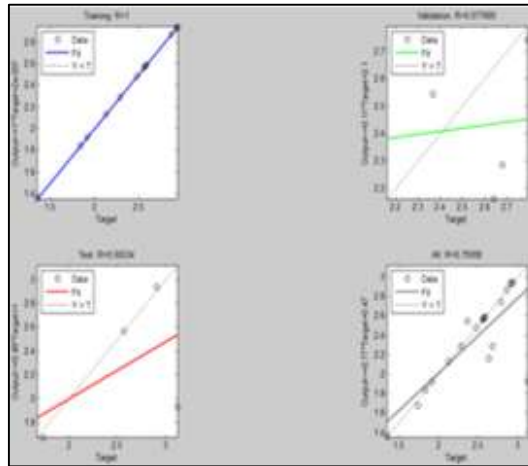
Figure 10: The measured values compared with predicted Ra for testing set

Table 10: Results predicted from training the net

| E. | Current | Al ₂ O ₃ Con. | Graphite Con. | Ra (µm) | |
|----|---------|-------------------------------------|---------------|----------|-----------|
| | | | | Measured | Predicted |
| 1 | 10 | 4 | 6 | 2.59 | 2.58 |
| 2 | 10 | 4 | 9 | 2.68 | 2.65 |
| 3 | 10 | 8 | 6 | 2.94 | 2.94 |
| 4 | 10 | 8 | 3 | 2.37 | 2.37 |
| 5 | 10 | 12 | 9 | 1.35 | 1.36 |
| 6 | 10 | 12 | 3 | 1.92 | 1.94 |
| 7 | 10 | 12 | 6 | 1.74 | 1.71 |
| 8 | 15 | 4 | 6 | 1.84 | 2.01 |
| 9 | 15 | 4 | 9 | 2.58 | 2.58 |
| 10 | 15 | 8 | 9 | 2.48 | 2.24 |
| 11 | 15 | 8 | 3 | 2.13 | 1.89 |
| 12 | 15 | 8 | 6 | 2.29 | 2.29 |
| 13 | 15 | 12 | 6 | 2.29 | 2.31 |
| 14 | 15 | 12 | 9 | 2.56 | 2.56 |
| 15 | 20 | 4 | 9 | 2.93 | 2.93 |
| 16 | 20 | 4 | 3 | 2.87 | 2.87 |
| 17 | 20 | 4 | 6 | 2.91 | 2.92 |
| 18 | 20 | 8 | 3 | 2.64 | 2.64 |
| 19 | 20 | 8 | 9 | 3.12 | 3.12 |
| 20 | 20 | 12 | 6 | 2.79 | 2.79 |
| 21 | 20 | 12 | 9 | 2.57 | 2.57 |

Table 11: Results predicted from testing the net

| E. | A | B | C | Ra (μm) | | Err % | ANN results | | |
|----|----|----|---|----------------------|-------|-------|-------------------|-------|--------|
| | | | | Meas. | Pred. | | $\bar{\phi}$ % | MSE | Acc. % |
| 1 | 10 | 4 | 3 | 2.46 | 2.59 | 5.28 | 4.98 | 0.016 | 95.02 |
| 2 | 10 | 8 | 9 | 2.69 | 2.59 | 3.72 | | | |
| 3 | 15 | 4 | 3 | 2.39 | 2.59 | 8.37 | | | |
| 4 | 15 | 12 | 3 | 2.14 | 2.23 | 4.21 | | | |
| 5 | 20 | 8 | 6 | 2.49 | 2.39 | 4.02 | | | |
| 6 | 20 | 12 | 3 | 2.81 | 2.93 | 4.27 | | | |

**Figure 11: Regression graphs for Ra**

5. Conclusions

1. The experimental advantage of this work is the use of obtained optimal variables to improve the material removal rate, reduces surface roughness, and less tool wear ratio of Carbon steel 304.
2. Metal removal rate or MRR at optimal inputs (i.e., A3B3C3) is maximized with maximizing current, AL₂O₃ and concentricity of graphite powder.
3. It was revealed that the surface roughness is proportional directly to discharge current, and inversely to the graphite powders concentricity, and AL₂O₃.
4. It was revealed that TWR is proportional inversely proportional to the AL₂O₃ and graphite powders concentricity and directly to discharge current.

References

- [1] S. Padhef, N. Nayak, S. K. Pandn, P. R. Dhal and S. S. Mahapatra, "Multi-objective parametric optimization of powder mixed electro-discharge machining using response surface methodology and non-dominated sorting genetic algorithm," Indian Academy of Sciences, Vol. 37, Part 2, pp. 223–240, April, 2012.
- [2] N. A. J. Hosni and M. A. Lajis "The influence of span-20 surfactant and micro-/nano- chromium (Cr) powder mixed electrical discharge machining (PMEDM) on the surface characteristics of AISI D2 hardened steel," IOP Conf. Series: Materials Science and Engineering 342, 2018.
- [3] K. Karunakaran and M. Chandrasekaran, "Experimental Investigation Nano Particles Influence in NPMEDM to Machine Inconel 800 with Electrolyte Copper Electrode," IOP Conf. Series: Materials Science and Engineering 197, 012068, 2017.
- [4] D. Rana, A. Kr. Pal and P. Tiwari, "Study of powder mixed dielectric in EDM-A review," International Journal of Engineering Science and advanced Research , Vol. 1, Issue 2, pp. 69-74, June, 2015.

- [5] K. H. Tseng, J. L. Chiu, H. L. Lee, C. Y. Liao, H. S. Lin, and Y. S. Kao1, "Preparation of Ag/Cu/Ti nanofluids by spark discharge system and its control parameters study," *Advances in Materials Science and Engineering*, Article ID 694672, 2015.
- [6] M. R. Abdul Razak, P. J. Liew, N. I. S. Hussein, Q. Ahsan and J. Yan, "Effect of surfactant and additives on electrical discharge machining of reaction bonded silicon carbide," *ARPN Journal of Engineering and Applied Sciences*, Vol. 12, No. 14, July, 2017.
- [7] R Boopathi, R Thanigaivelan and M Prabu, "Effects of process parameters on MRR, EWR and Ra in nanoparticles mixed EDM," *Research & Development in Material Science*, 2018.
- [8] H. Oktem, T. Erzurumlu and F. Erzincanli, "Prediction of minimum surface roughness in end milling mold parts using neural network and genetic algorithm," *Materials and Design*, vol. 27, pp.735–744, 2006.
- [9] B. Ozcelik, H. Oktem and H. Kurtaran, "Optimum surface roughness in end milling inconel 718 by coupling neural network model and genetic algorithm," *Int J Adv Manuf Technol*, vol. 27, pp. 234–241, 2005.